MEF2C phosphorylation is required for chemotherapy resistance in acute myeloid leukemia

Fiona C Brown[1], Eric Still[1], Richard P Koche[2], Christina Y Yim[1], Sumiko Takao[1], Paolo Cifani[1], Casie Reed[1], Shehana Gunasekera[1], Scott B Ficarro[3], Peter Romanienko[4], Willie Mark[4], Craig McCarthy[1], Elisa de Stanchina[1], Mithat Gonen[5], Venkatraman Seshan[5], Patrick Bhola[6], Conor O'Donnell[1], Barbara Spitzer[7], Crystal Stutzke[8], Vincent-Philippe Lavallée[9,10], Josée Hébert[9-12], Andrei V Krivtsov[2,13], Ari Melnick[14], Elisabeth M Paietta[15], Martin S Tallman[16], Anthony Letai[6,17], Guy Sauvageau[9-12], Gayle Pouliot[6], Ross Levine[2,7,16,18], Jarrod A Marto[3], Scott Armstrong[2,13], Alex Kentsis[1,7,14]

SUPPLEMENTARY METHODS

Reagents

All reagents were obtained from Sigma Aldrich unless otherwise stated. Synthetic oligonucleotides were obtained from Eurofins MWG Operon (Hunstville, AL, USA) and purified by HPLC. Synthetic ultramer oligonucleotides for CRISPR/Cas9 mouse genome engineering were obtained from Integrated DNA Technologies (Coralville, IA). DNA Sanger sequencing was performed by Genewiz (South Plainfield, NJ, USA).

Plasmids and expression vectors

Human full-length *MEF2C* cDNA isoform 1 (RefSeq ID: NM_002397.4) was cloned into the pMSCV-IRES-tdTomato (MIT) retroviral expression vector, kindly provided by Scott Armstrong (1), to generate *MIT-MEF2C*. pRecLV105 lentiviral vector (GeneCopoeia, Rockville, MD, USA) was used to generate pRecLV105-*MEF2C*. The doxycycline-inducible pINDUCER20 lentiviral expression vector was a kind gift from Thomas Westbrook (2), and used to generate pINDUCER20-*MEF2C* using Gateway cloning according to the manufacturer's instructions (Fisher Scientific, Waltham, MA, USA). Site-directed mutagenesis was used to generate *MEF2C S222A* and *MEF2C S222D* according to the manufacturer's instructions (QuikChange Lightning, Agilent, Santa Clara, CA, USA). Human full-length *MARK3* cDNA isoform c (RefSeq ID: NM_2376.6) was amplified from the OCI-AML2 human AML cell line and cloned using Gateway cloning into pLX304 (3). Lentivirus packaging vectors psPAX2 (Addgene plasmid #12260) and pMD2.G (Addgene plasmid #12259) were a gift from Didier Trono, and ecotropic retroviral packaging vector pCL-Eco was a gift from Inder Verma (Addgene plasmid #12371) (4). The MSCV-IRES-GFP *MLL-AF9* expression vector was provided by Scott Armstrong (5). The MSCV HoxA9-IRES-Meis PGK-Neo expression vector was used as previously described (6).

shRNA vectors targeting MARK3 (TAAATTTAGATCTTGCTTCTTT and TTAATTTACATCATAATCACTG) were cloned into pLT3REVIR, kindly provided by Scott Lowe (7).

Generation of *Mef2c*^{S222A} and *Mef2c*^{S222D} Mice

Generation of knock-in *Mef2c*^{S222A} and *Mef2c*^{S222D} mutant mice using CRISPR/Cas9 genome editing and homologous recombination. A CRISPR gRNA targeting exon 5 of the *Mef2c* gene was designed (GGAATGGATACGGCAACCCC) and expressed *in vitro* using the approach previously described (8). The donor templates for recombination were designed according to Wefers and colleagues (9). For *Mef2c*^{S222A}, we used the oligonucleotide ATATGAGCTGTTCTTTAAAAACATGCACACGCCTCGATTTCTCCCTGAGTTTTGTCATCTCT TGTGTTAACAGGGAATGGATACGGCAACCCCCCG**c**AAC**g**C**g**CCAGGCCTGCTGGTCTCACC TGGTAACCTGAACAAGAATATACAAGCCAAATCTCCTCCCCCTATGAATCTAGGAATGAATA ATCGTA, where lowercase nucleotides indicate in-frame substitutions from the reference sequence and underlined regions indicates the addition of a HhaI and AciI restriction sites, respectively. For *Mef2c*^{S222D}, we used the oligonucleotide ATATGAGCTGTTCTTTAAAAACATGCACACGCCTCGATTTCTCCCTGAGTTTTGTCATCTCT TGTGTTAACAGGGAATGGATACGGCAACCCCCCG**c**AAC**gat**CCAGGCCTGCTGGTCTCACCT GGTAACCTGAACAAGAATATACAAGCCAAATCTCCTCCCCCTATGAATCTAGGAATGAATAA TCGTA, where lowercase nucleotides indicate in-frame substitutions from the reference sequence and underlined regions indicates the addition of a Sau3A and AciI restriction sites, respectively. Mouse zygotes from C57BL/6J:CBA F2 hybrids were injected with 100 ng/µl of gRNA, 50 ng/µl Cas9 mRNA and 50 ng/µl of donor oligonucleotide into the pronucleus. Founder mice were first screened using restriction endonuclease digestion of genomic DNA isolated from tail tissues. Digestions were carried out using HhaI and AciI for Mef2c^{S222A} and Sau3A and AciI

for Mef2c^{S222D} alleles. The positive mice were then analyzed by DNA sequencing of PCR products obtained from amplifying the targeted region of exon 5 using the following forward and reverse primers, respectively: GTATGACTCACAGCTAGGCGTATC, and CATCGTGTTCTTGCTGCCAGGTG. Founder mice of both *Mef2c*^{S222A} and *Mef2c*^{S222D} mutants were back-crossed to wild-type C57BL/6J mice for at least two generations before use. For all experiments using *Mef2c* knock-in mutant animals, mice of 8-12 weeks of age were used and wild-type litter mates were used as controls. No blinding was done in any *in vivo* animal studies or in data analysis.

Cell culture

Human AML cell lines were cultured in RPMI-1640 medium supplemented with 10% fetal bovine serum (FBS) and antibiotics (100 U / ml penicillin and 100 µg / ml streptomycin) in a humidified atmosphere at 37 °C and 5% CO_2. HEK293T cells were cultured in Dulbecco's Modified Eagle medium (DMEM) supplemented with 10% FBS and antibiotics (100 U / ml penicillin and 100 µg / ml streptomycin). Short-term culture of patient AML specimens were performed by thawing viably preserved cells in IMDM supplemented with 10% FBS, 0.1 mM β-mercaptoethanol, and 100 ng/ml human SCF, 20 ng/ml human IL3, 20 ng/ml human G-CSF, and 50 ng/ml human FLT3-L (all obtained from Peprotech, Rocky Hill, New Jersey, USA).

Virus production and cell transduction

Lentiviral production was performed as previously described (10). Briefly, HEK293T packaging cells were transfected with TransIT-LTI according to the manufacturer's instructions (Mirus Bio LLC, Madison, WI, USA). For lentiviral expression vectors, a 2:1:1 ratio of the expression vector, packaging and pseudotyping plasmids was used. For retroviral expression

vectors, a 1:1 ratio of expression vector to pCL-Eco packaging plasmid was used. Viral supernatant was collected at 48 and 72 hours post-transfection, pooled, filtered, concentrated by centrifugation using the Amicon Ultra-15 Centrifugal Filter Units (EMD Millipore, Darmstadt, Germany) and stored at -80 °C. HEK293T cells were transduced by spin infection with pRecLV105 or pLX304 viral particles at a multiplicity of infection (MOI) of 1 in the presence of 8 µg/ml polybrene, and transduced cells were selected with 2 µg/ml puromycin for 3 days (for pRecLV105) or 10 µg/ml blasticidin (for pLX304) for 8 days. Human AML cell lines were transduced by spin infection with viral particles at a MOI of 1, and transduced cells were selected with 2 mg/ml G418 sulfate (for pINDUCER20) for 14 days or Venus positive cells were isolated by FACS (for pLT3REVIR). Mouse hematopoietic progenitor cells were transduced with viral particles at MOI of 20 by spin infection on retronectin-treated tissue culture plates (Takara Bio USA, Inc; Mountain View, CA, USA) and GFP or tdTomato positive cells were isolated by FACS 3 days after transduction (for MSCV-IRES-GFP/Tomato) or 0.5 mg/ml G418 (for MSCV-IRES-PGK-NEO) for 6 days.

Isolation of mouse hematopoietic progenitor cells

Femurs and tibias were dissected from 8-12 week-old C57BL/6J or transgenic mice, and cells were extracted using mortar and pestle crushing, and mesh filtration. Red blood cells were lysed using the RBC Lysis Buffer according to the manufacturer's instructions (BioLegend, San Diego, CA, USA). Progenitor cells were isolated using lineage depletion with the Mouse Lineage Depletion Kit according to the manufacturer's instructions (MACS Miltenyi Biotech, Bergisch Gladbach, Germany). Isolated cells were subsequently stained with the following antibodies for isolation of granulocyte/macrophage progenitor cells (GMP): Sca-1, CD16/32, CD117 and CD34. Fluorescence-activated cell sorting was performed using the BD FACSAria (Becton Dickinson, San Jose, CA) and FACS analysis was done using FlowJo software (FlowJo,

Ashland, Oregon, USA). Sorted GMP cells were cultured overnight in IMDM supplemented with 15% FBS, 100 U / ml penicillin and 100 µg / ml streptomycin, and 50 ng/ml mouse SCF, 10 ng/ml mouse IL-3, and 10 ng/ml mouse IL-6 (all from Peprotech). Antibodies used in flow cytometry are detailed in Table S5.

Limiting dilution transplants

Leukemic cells harvested from the bone marrow of moribund *MLL-AF9;MEF2C* animals were transplanted by intravenous injection into sub-lethally irradiated (600 rad) C57BL/6J mice at cell doses indicated throughout the text. Leukemia stem cell frequency was determined using ELDA software (11).

Isolation of CD34 cells

Mononuclear cells were isolated from cord blood as previously described (12). Cells were cultured short-term in IMDM supplemented with 10% FBS, 0.1 mM β-mercaptoethanol, and 100 ng/ml human SCF, 20 ng/ml human IL3, 20 ng/ml human G-CSF, and 50 ng/ml human FLT3-L (all obtained from Peprotech).

Cell proliferation studies

For human AML cell lines transduced with pINDUCER20-*MEF2C,* pINDUCER-*MEF2C-S222A* and pINDUCER-*MEF2C-S222D*, 1 x 10^4 cells were incubated in 0.1 ml with 600 ng/ml of doxycycline for 72 hours in 96-well plates. For chemotherapy treatments, cytarabine and doxorubicin dissolved in PBS were added to cells after 24 hours of doxycycline treatment. Cell growth was assessed using the Cell Titer-Glo Luminescent Viability assay (Promega, Madison,

WI, USA), as measured using luminescence on the Infinite M1000Pro plate reader using integration time of 250 milliseconds (Tecan, Männedorf, Switzerland). For assays using patient AML cells, cells were assessed by FACS using the BD FACSCanto II cytometer (BD Biosciences) after staining cells with human CD45, mouse CD45 and DAPI viability stain. Antibodies used in flow cytometry are detailed in Table S5.

Clonogenic assays

All colony forming assays were performed using HSC001 methylcellulose medium, according to the manufacturer's instructions (R&D Systems, Minneapolis, MN, USA). For GMP cells transduced with *MLL-AF9*, 1,000 cells/replicate were plated in 1.27% final concentration methylcellulose with IMDM supplemented with 10% FBS and mouse cytokines (10 ng/ml IL-3, 10 ng/ml IL-6 and 20 ng/ml SCF). Leukemia blast colonies were counted after 7 days. For re-plating experiments, cells were pooled, counted and replated at the same density. Purified GMP cells (20,000 cells/replicate) from the *Mef2c*^{S222A} and *Mef2c*^{S222D} transgenic mice were plated in 1.27% final concentration methylcellulose with IMDM supplemented with 10% FBS and mouse cytokines (10 ng/ml IL-3, 10 ng/ml IL-6 and 50 ng/ml SCF). Colonies from CFU-G, CFU-G and CFU-GM units were counted after 14 days.

Transcriptional reporter assays

MEF2C transcriptional activity was quantified using the Cignal MEF2 reporter assay, using the CTAGCGCTCTAAAAATAACCCT response element, according to the manufacturer's instructions (Qiagen, Hilden, Germany). For K562 and HEK-293T experiments, cells were either electroporated according to the manufacturer's instructions (Neon Transection System,

Invitrogen) or transfected with the MEF2C reporter gene using the Fugene transfection reagent (Promega) and detected using the Dual-Glo Luciferase Assay System (Promega), according to the manufacturer's instructions. MEF2C transcriptional activity was calculated using the ratios of the firefly/*Renilla* signals, and normalized to the internal positive control for the reporter assay.

Recombinant kinase screen

The protein kinase screen was performed using a recombinant serine kinase library as previously described (13). Briefly, 172 serine/threonine kinases (Supplementary Data 6) were individually expressed as N-terminal GST-fusion proteins in insect cells, and purified using glutathione sepharose chromatography. A synthetic peptide corresponding to phosphoserine 222 for human MEF2C (RefSeq ID: NM_002397.4) Ac-GNPRN[pS]PGLLVC-NH2 was synthesized (Tufts University, Medford, MA, USA), purified by HPLC, and confirmed by mass spectrometry. For the screen, the MEF2C peptide was dissolved in DMSO at 10 μM, 1 μM, and 0.1 μM, and specific kinase activity on respective substrates was determined by the off-chip mobility shift assay (MSA) using the LabChipTM3000 instrument (Caliper Life Sciences, Hopkinton, MA, USA). The kinase reaction was analyzed by the product ratio, which was calculated from the peak heights of the kinase substrate (K) and MEF2C (M) peptides (K/(K+M)). Additional protein kinases were assayed using the immobilized metal ion affinity-based fluorescence polarization (IMAP) system, where the kinase reaction was evaluated by the fluorescence polarization at 485 nm for excitation and 530 nm for emission. Staurosporine was used as the positive control for almost all kinases and the readout of this was set as 0% inhibition, with the readout value of no kinase set as a 100% inhibition. Inhibition of 20% or more was used to score positive signals.

Western immunoblotting

Primary human or mouse leukemia cells were lysed in 100 µl of lysis buffer containing 30 mM Tris HCl, 1% sodium dodecyl sulfate (SDS), 7% glycerol, 1.25% beta-mercaptoethanol, 0.2 mg/ml Bromophenol Blue, pH 6.8 per 1 million cells and incubated at 95 °C for 10 minutes. Human AML cell lines and HEK293T cells were lysed in RIPA buffer (15 mM NaCl, 1% NP-40, 0.5% sodium deoxycholate, 0.1% SDS, 50 mM Tris, pH 8.0) and sonicated using the Covaris S220 adaptive focused sonicator, according to the manufacturer's instructions (Covaris, Woburn, CA). Lysates were cleared by centrifugation at 11,000 x g for 10 minutes at 4 °C and clarified lysates were denatured in Laemmli sample buffer at 95 °C for 10 minutes. For phosphatase treatment, cell lines were lysed in RIPA buffer without SDS and treated with 800 units of λ phosphatase (P9614) and 6500 units of alkaline phosphatase (P0114) for 30 minutes before the addition of 1% SDS. For DSS treatment, cells were treated with increasing amounts of DSS according to the manufacturer's instructions prior to lysis. Lysates were separated by sodium dodecyl sulfate polyacrylamide gel electrophoresis (SDS-PAGE) and transferred onto an Immobilon-FL PVDF membrane (EMD Millipore, Darmstadt, Germany). Membranes were blocked with the Odyssey Blocking Buffer (Li-Cor, Nebraska, USA) and blotted with primary antibodies for MEF2C (1:1000), pS222 MEF2C (1:1000), MARK3 (1:1000) or beta-actin (1:1000), followed by blotting with goat IRDye 680 RD anti-rabbit and IRDye 800 CW anti-mouse secondary antibodies. For peptide competition assays, pS222 MEF2C was pre-blocked with synthetic peptides for phospho-MEF2C and nonphospho-MEF2C corresponding to amino acids surrounding S222. Signals were recorded and quantified using the Odyssey CLx fluorescence scanner (Li-Cor, Nebraska, USA). Antibodies used for Western blotting are detailed in Table S5.

Flow cytometry

Antibodies used in flow cytometry are detailed in Table S5. For analysis of annexin V, cells were washed and resuspended in annexin V binding buffer (10 mM HEPES, pH 7.4, 140 NaCl, 2.5 mM $CaCl_2$). Cells were stained with annexin V for 15 minutes at room temperature in the dark, with the addition of DAPI before analysis by flow cytometry. For analysis of caspase 3 cleavage, cells were fixed with BD Cytofix/Cytoperm buffer according to the manufacturer's protocol (BD Biosciences). Fixed cells were stained with Alexa Fluor 647-conjugated anti cleaved caspase-3 (BD Biosciences) in BD Perm/Wash Buffer (BD Biosciences) for 30 minutes at room temperature in the dark. Bone marrow mononuclear cells were assessed using the surface cell marker antibodies B220, Gr-1, CD11b, CD4 and CD8. Flow cytometry was analyzed on a BD LSRFortessa and FlowJo software.

BH3 profiling

OCI-AML2 cells transduced with pINDUCER20-*MEF2C* and pINDUCER-*MEF2C-S222A* were incubated with 600 ng/ml of doxycycline for 48 hours prior to BH3 profiling. BH3 profiling was performed as previously described (14). Flow cytometry was analyzed on a BD FACSCanto II cytometer and FlowJo software.

Giemsa staining

Dip Quick Stain (J-322, Jorgensen Laboratories, Inc) was used according to the manufacturer's protocol for Giemsa staining of peripheral blood smears and bone marrow cytospins. Cytospins of bone marrow cells were prepared using a benchtop Cytospin Centrifuge (Thermo Fisher Scientific) of 2 x 10^5 cells in PBS onto Superfrost Plus microscope slides, according to the manufacturer's instructions (Thermo Fisher Scientific).

Quantitative RT-PCR

RNA was extracted using TRIzol Reagent (Thermo Fisher Scientific, Waltham, MA) followed by the Qiagen RNeasy Mini Kit according to the manufacturer's instructions. Complementary DNA was synthesized using the SuperScript III First-Strand Synthesis system according to the manufacturer's instructions (Invitrogen, Carlsbad, California). Quantitative real-time PCR was performed using the KAPA SYBR FAST PCR polymerase, according to the manufacturer's instructions (Kapa Biosystems, Wilmington, MA, USA). Ct values were calculated using ROX normalization on the ViiA 7 software (Applied Biosystems).

Sequences for RT-qPCR primers

Gene	Forward (5' – 3')	(Reverse 5' – 3')
Human *MEF2C*	TCACTGGGAAACCCCAACCTAT	TGCCTGCACCAGACGTGAGG
Human *GAPDH*	AATCCCATCACCATCTTCCA	TGGACTCCACGACGTACTCA
Mouse *Hdac7*	CCCACCTGTCAGACCCAAGT	AGTCATAGACCAGCCCTGTAGCA
Mouse *Nr4a1*	GCACAGCTTGGGTGTTGATG	CAGACGTGACAGGCAGCTG
Mouse *c-Jun*	CCAAGTGCCGGAAAAGGAA	GCCACCTGTTCCCTGAGCAT
Mouse *Gapdh*	AGAACATCATCCCTGCATCCA	CAGATCCACGACGGACACATT

Gene expression profiling

OCI-AML2 cells transduced with pINDUCER20-*MEF2C* and pINDUCER-*MEF2C-S222A* were incubated with 600 ng/ml of doxycycline for 48 hours. For MRT199665 treatment studies, OCI-AML2 cells were treated with 100 nM MRT199665 or DMSO vehicle control for 48 hours. RNA was extracted from cells from 3 biological replicates as described above. The quality of

RNA was verified on the Agilent Bioanalyzer 2100 platform (Agilent, Santa Clara, CA, USA). For RNA sequencing, a Poly-A tail library selection was performed. Sequencing was done using the Illumina HiSeq platform (Illumina, San Diego, CA) with 30-45 million 50bp, paired-end reads.

ATAC-seq

ATAC-seq was performed as previously described (15). For cells, nuclei from 200,000 OCI-AML2 cells transduced with pINDUCER20-*MEF2C* and pINDUCER-*MEF2C-S222A* and incubated with 600 ng/ml of doxycycline for 48 hours (in triplicate) were treated with 2.5 µl of transposase (Illumina) for 37 °C, 30 minutes. Following DNA purification and DNA library preparation, the quality of DNA was verified using the Agilent Bioanalyzer 2100 platform. Sequencing was done using the Illumina HiSeq platform with 30-45 million 50bp, paired-end reads.

Data Analysis

RNA-seq raw reads were quality and adapter trimmed using 'trim_galore' before aligning to human assembly hg19 with STAR v2.5 using the default parameters. Coverage and post-alignment quality were assessed using the Picard tool CollectRNASeqMetrics (http://broadinstitute.github.io/picard/). Read count tables were created using HTSeq v0.6.1. Normalization and expression dynamics were evaluated with DESeq2 using the default parameters. Gene set enrichment analysis (GSEA, http://software.broadinstitute.org/gsea/) was performed with the pre-ranked option and default parameters. The log2 fold change from DESeq2 was used as input, and tested against all gene sets in MSigDB version 5.1. ATAC-seq reads were similarly filtered for quality and adapter sequences and aligned to hg19 using bowtie2 (v2.2.2). Enriched regions were discovered using MACS2 and compared with input

sequence (fold change > 2, FDR-adjusted $p < 0.01$) and filtered for blacklisted regions (http://mitra.stanford.edu/kundaje/akundaje/release/blacklists/). Signal was normalized to sequencing depth and both gene associations and motif signatures were detected with Homer ('annotatePeaks.pl' and 'findMotifsGenome.pl', respectively). Clustering was accomplished using partitioning around medoids (PAM) for k=3, and displayed as row-scaled z-scores. For *MARK1-4* gene expression, raw sequences of transcriptome data collected as part of the Cancer Genome Atlas (TCGA) from 138 patients with AML (16) were aligned to the NCBI37/mm9 human reference genome using STAR and differential expression analysis obtained using the DESeq2 Bioconductor algorithm.

For analysis of phosphoproteomics data, the normalized phosphorylated peptide levels for each of the 8 samples were used in differential expression analysis and expression levels in the remission group were compared to those in induction failure group using a two sample t-test. An empirical Bayes approach was used to shrink the peptide specific sample variances towards a common value (17) to obtain a moderated t-statistic for assessing the extent of differential expression. Statistical methodology was described previously (18) which was implemented in the limma R package (19,20).

For the validation cohort used in this study, a univariate analysis was performed on variables that were observed in 5 patients or more. The two variables with the lowest p-values were included in a multivariate model. Proteomics and genomics data have been deposited to MassIVE (MassIVE ID MSV000080646, https://massive.ucsd.edu/) and Gene Expression Omnibus (GEO series number GSE94453, https://www.ncbi.nlm.nih.gov/geo/), respectively.

Primary AML patient cohorts

The E1900 ECOG cohort of young adult AML has been previously described (21). Gene expression data were subjected to quantile normalization and log-transformed. Association between expression and survival were evaluated using a Cox model and Kaplan-Meier plots.

The Leucegene 415 AML patient cohort and methodology for RNA-sequencing have been described previously (22). Clinical outcomes were assessed among the 263 patients with *de novo* AML, excluding acute promyelocytic leukemia, who received standard intensive therapy. Definitions of complete remission (CR), relapse-free survival (RFS) and overall survival (OS) followed ELN recommendations (23). Kaplan Meier Curves for OS and RFS were generated in R version 3.2.3 using the survival package and p-values were calculated using the survdiff function. Differences in CR rates were calculated using two-tailed Fisher's exact test (Graphpad QuickCalcs). Quantiles were used to define patient groups with low and high expression for *MARK3*, and the < 75th vs > 75th percentile were compared.

SUPPLEMENTAL REFERENCES

1. Zhu N, Chen M, Eng R, DeJong J, Sinha AU, Rahnamay NF*, et al.* MLL-AF9- and HOXA9-mediated acute myeloid leukemia stem cell self-renewal requires JMJD1C. *The Journal of clinical investigation* **2016**;126:997-1011.
2. Meerbrey KL, Hu G, Kessler JD, Roarty K, Li MZ, Fang JE*, et al.* The pINDUCER lentiviral toolkit for inducible RNA interference in vitro and in vivo. *Proceedings of the National Academy of Sciences of the United States of America* **2011**;108:3665-70.
3. Yang X, Boehm JS, Yang X, Salehi-Ashtiani K, Hao T, Shen Y*, et al.* A public genome-scale lentiviral expression library of human ORFs. *Nature methods* **2011**;8:659-61.
4. Naviaux RK, Costanzi E, Haas M, Verma IM. The pCL vector system: rapid production of helper-free, high-titer, recombinant retroviruses. *Journal of virology* **1996**;70:5701-5.
5. Krivtsov AV, Twomey D, Feng Z, Stubbs MC, Wang Y, Faber J*, et al.* Transformation from committed progenitor to leukaemia stem cell initiated by MLL-AF9. *Nature* **2006**;442:818-22.
6. Lehnertz B, Pabst C, Su L, Miller M, Liu F, Yi L*, et al.* The methyltransferase G9a regulates HoxA9-dependent transcription in AML. *Genes & development* **2014**;28:317-27.

7. Zuber J, McJunkin K, Fellmann C, Dow LE, Taylor MJ, Hannon GJ*, et al.* Toolkit for evaluating genes required for proliferation and survival using tetracycline-regulated RNAi. *Nature biotechnology* **2011**;29:79-83.
8. Romanienko PJ, Giacalone J, Ingenito J, Wang Y, Isaka M, Johnson T*, et al.* A Vector with a Single Promoter for In Vitro Transcription and Mammalian Cell Expression of CRISPR gRNAs. *PloS one* **2016**;11:e0148362.
9. Wefers B, Ortiz O, Wurst W, Kuhn R. Generation of targeted mouse mutants by embryo microinjection of TALENs. *Methods* **2014**;69:94-101.
10. Kentsis A, Reed C, Rice KL, Sanda T, Rodig SJ, Tholouli E*, et al.* Autocrine activation of the MET receptor tyrosine kinase in acute myeloid leukemia. *Nature medicine* **2012**;18:1118-22.
11. Hu Y, Smyth GK. ELDA: extreme limiting dilution analysis for comparing depleted and enriched populations in stem cell and other assays. *Journal of immunological methods* **2009**;347:70-8.
12. Ramaswamy K, Forbes L, Minuesa G, Gindin T, Brown F, Kharas MG*, et al.* Peptidomimetic blockade of MYB in acute myeloid leukemia. *Nature communications* **2018**;9:110.
13. Kitagawa D, Gouda M, Kirii Y, Sugiyama N, Ishihama Y, Fujii I*, et al.* Characterization of kinase inhibitors using different phosphorylation states of colony stimulating factor-1 receptor tyrosine kinase. *Journal of biochemistry* **2012**;151:47-55.
14. Ryan J, Montero J, Rocco J, Letai A. iBH3: simple, fixable BH3 profiling to determine apoptotic priming in primary tissue by flow cytometry. *Biol Chem* **2016**;397:671-8.
15. Buenrostro JD, Giresi PG, Zaba LC, Chang HY, Greenleaf WJ. Transposition of native chromatin for fast and sensitive epigenomic profiling of open chromatin, DNA-binding proteins and nucleosome position. *Nature methods* **2013**;10:1213-8.
16. Cancer Genome Atlas Research N. Genomic and epigenomic landscapes of adult de novo acute myeloid leukemia. *The New England journal of medicine* **2013**;368:2059-74.
17. Smyth GK. Linear models and empirical bayes methods for assessing differential expression in microarray experiments. *Stat Appl Genet Mol Biol* **2004**;3:Article3.
18. Phipson B, Lee S, Majewski IJ, Alexander WS, Smyth GK. Robust Hyperparameter Estimation Protects against Hypervariable Genes and Improves Power to Detect Differential Expression. *Ann Appl Stat* **2016**;10:946-63.
19. Team RC. R: A language and environment for statistical computing. *R Foundation for Statistical Computing* **2017**.
20. Ritchie ME, Phipson B, Wu D, Hu Y, Law CW, Shi W*, et al.* limma powers differential expression analyses for RNA-sequencing and microarray studies. *Nucleic Acids Res* **2015**;43:e47.
21. Patel JP, Gonen M, Figueroa ME, Fernandez H, Sun Z, Racevskis J*, et al.* Prognostic relevance of integrated genetic profiling in acute myeloid leukemia. *The New England journal of medicine* **2012**;366:1079-89.
22. Lavallee VP, Baccelli I, Krosl J, Wilhelm B, Barabe F, Gendron P*, et al.* The transcriptomic landscape and directed chemical interrogation of MLL-rearranged acute myeloid leukemias. *Nat Genet* **2015**;47:1030-7.
23. Dohner H, Estey E, Grimwade D, Amadori S, Appelbaum FR, Buchner T*, et al.* Diagnosis and management of AML in adults: 2017 ELN recommendations from an international expert panel. *Blood* **2017**;129:424-47.

SUPPLEMENTARY FIGURE LEGENDS

Supplementary Figure S1.

MEF2C phosphorylation is identified in a phosphoproteomic screen for primary chemoresistance.

A, Distribution of differentially expressed phosphorylated proteins in diagnostic AML specimens with primary chemotherapy resistance and induction failure as compared to complete induction remission. **B,** MS1 plots of pS222 MEF2C. **C,** Protein sequence alignment of the MEF2 isoforms at the sequence surrounding S222 of MEF2C (shown in red). Isoform 1 has been used for each alignment.

Supplementary Figure S2.

pS222 MEF2C is associated with chemoresistance in primary AML

A) Peptide competition Western immunoblot of OCI-AML2 cells for pS222 MEF2C. P = phosphorylated MEF2C peptide at S222; NP = non-phosphorylated MEF2C peptide at S222. **B,** Peptide competition Western immunoblot for pS222 MEF2C of HEK293T cells lentivirally transduced with wild-type MEF2C. **C,** Lysates prepared from HEK293T cells lentivirally transduced with wild-type MEF2C were treated with (+) or without (-) λ phosphatase (800 units) and immunoblotted for pS222 MEF2C. Arrows indicate pS222 MEF2C. Western blot analysis for MEF2C and pS222 MEF2C in pediatric **D, F,** and adult **E, G,** age, disease and therapy-matched patient AML specimens with induction failure and complete remission. The human AML cell lines OCI-AML2 and U937 were used as positive and negative controls for MEF2C expression, respectively. **H,** Normalized $\log_2$ expression of total MEF2C and pS222 MEF2C compared to actin in induction failure and complete remission AML patient specimens. Median expression of pS222 MEF2C for the cohort is indicated (blue dashed line). * and ** $p = 6.0 \times 10^{-3}$ and 6.5×10^{-4} for MEF2C and pS222 MEF2C in induction failure versus relapse and remission respectively (t-test). **I,** Normalized $\log_2$ expression of pS222 MEF2C compared to total MEF2C in induction failure and complete remission AML patient specimens ($p = 0.71$, t-test). **(J)** Normalized $\log_2$ expression of MEF2D as compared to actin in induction failure and complete remission AML patient specimens ($p = 0.98$, t-test). **K,** Kaplan-Meier survival curves for the ECOG E1900 AML cohort based on highest expression quartile for MEF2C vs others ($p = 3.8 \times 10^{-2}$, log-rank test).

Supplementary Figure S3.

Mef2c phosphorylation is dispensable for normal hematopoiesis but required for the development of MLL-AF9 leukemia *in vivo*.

A, Sequencing electropherograms of tail genomic DNA from *Mef2c*^{S222A} and *Mef2c*^{S222D} mice at the *Mef2c* locus. CRISPR/Cas9-induced genome editing introduces c.TCA>GCG (S222A) and c.TCA>GAT (S222D) mutations, and restriction enzyme sequencing sites, as underlined red and black, respectively. **B,** Mendelian ratios from heterozygous intercrosses for *Mef2c*^{S222A} and

Mef2c^{S222D} mice. Error bars represent standard deviation of the mean. Body size **C,** and weight **D,** is preserved in *Mef2c*$^{S222A/S222A}$ and *Mef2c*$^{S222D/S222D}$ mice compared to wild-type litter mate controls. Error bars represent standard deviation of the mean of 5 mice per group. **E,** Representative micrographs of peripheral blood smears from *Mef2c*$^{S222A/S222A}$ and *Mef2c*$^{S222D/S222D}$ mice. Scale bar denotes 50 µm. **F,** Enumeration of hemoglobin (Hb), red blood cells (RBC), white blood cells (WBC) and platelets (PLT) in peripheral blood from *Mef2c*$^{S222A/S222A}$ and *Mef2c*$^{S222D/S222D}$ mice compared to wild-type litter mates. Error bars represent standard deviation of the mean of 6 animals per genotype. **G,** Representative images of Wright-Giemsa-stained cytospin preparations of bone marrow cells from *Mef2c*$^{S222A/S222A}$ and *Mef2c*$^{S222D/S222D}$ mice. Scale bar denotes 50 µm. **H,** Colony formation of GMP cells from *Mef2c*$^{S222A/S222A}$ and *Mef2c*$^{S222D/S222D}$ mice. Error bars represent standard deviation of the mean of 3 biological replicates. Abbreviations: colony-forming units granulocyte/macrophage (CFU-GM); colony-forming units granulocyte (CFU-G); colony-forming units granulocyte/macrophage (CFU-M) **I,** Schematic of competitive transplant. **J,** Representative FACS plot of peripheral blood mononuclear cell CD45.2 mutant and CD45.1 wild-type cells 4 weeks following competitive transplantation. **K,** Serial replating clonogenic efficiencies of bone marrow granulocyte-macrophage progenitor cells from an independent mouse strain compared to Figure 2G for *Mef2c*$^{S222A/S222A}$, *Mef2c*$^{S222D/S222D}$ and wild-type litter mates transduced with *MLL-AF9*. Error bars represent standard deviation of the mean of 3 biological replicates. Below, representative micrographs of colonies at day 7. Scale bar denotes 100 µm. *, ** and *** $p = 8.7 \times 10^{-4}$, 1.2×10^{-4} and 6.2×10^{-4} of *WT;MLL-AF9* versus *S222A/S222A;MLL-AF9,* t-test. **L,** Schematic for *in vivo Mef2c*^{S222A} and *Mef2c*^{S222D}*;MLL-AF9* experiments. **M,** Representative FACS plot analysis of bone marrow cells collected from primary recipient animals transplanted as shown in **L**. Wild-type (WT) and *Mef2c*$^{S222D/S222D}$ cells were collected from moribund animals. *Mef2c*$^{S222A/S222A}$ cells were collected from bone marrow aspirates 170 days after transplant.

Supplementary Figure S4.

MEF2C phosphorylation is required for leukemia stem cell survival and maintenance

A, Schematic for *in vivo MLL-AF9* and *MEF2C* initiation/maintenance experiments. **B,** Western blot analysis for MEF2C and pS222 MEF2C in primary leukemia cells shown in **A**. Below, quantitative analysis of MEF2C and pS222 MEF2C, as measured using quantitative fluorescence immunoblotting, and normalized to actin, demonstrating significantly reduced abundance of pS222 MEF2C in S222A. (*$p = 5.8 \times 10^{-5}$ for MEF2C S222A versus MEF2C, t-test). Error bars represent standard deviation of the mean for 3 biological replicates. **C,** Colony formation of primary leukemia cells shown in **B**. Below, representative micrographs of colonies at day 7. *** $p = 5.1 \times 10^{-5}$ S222A vs MEF2C, t-test. Error bars represent standard deviation of the mean of 3 biological replicates. Scale bar denotes 100 µm. **D,** Cleaved-caspase 3 analysis of primary leukemia cells shown in **B**. Error bars represent standard deviation of the mean of 3 biological replicates. * $p = 0.025$ S222A vs MEF2C, t-test. **E,** Kaplan–Meier survival curves of primary recipient mice transplanted with wild-type *MLL-AF9;MEF2C*, dominant negative *MLL-AF9;MEF2C S222A* or control *MLL-AF9;MIT* transformed leukemias. N = 10 animals in each group. Kaplan–Meier survival curves of secondary recipient mice transplanted with **F,** 10,000

cells, **G,** 1,000 cells and **H,** 10 cells from that shown in **E**. N = 20 animals in each group. p = 0.02 S222A vs MEF2C for 10,000 cells; 4.3 x 10^{-4} S222A vs MEF2C for 1,000 cells; 4.4 x 10^{-2} S222A versus MEF2C for 10 cells, log-rank test. qRT-PCR of **I,** *Hdac7,* **J,** *Nr4a1,* **K,** *c-Jun* and **L,** *Cebpa* in primary *MLL-AF9;MEF2C* transformed cells. Error bars represent standard deviation of the mean for 3 biological replicates.

Supplementary Figure S5.

MEF2C phosphorylation is required for leukemia stem cell survival and maintenance

A, Schematic for *in vivo Runx1$^{-/-}$;Flt3^{ITD}* and *MEF2C* leukemia experiments. **B,** Western immunoblot analysis for MEF2C and pS222 MEF2C in secondary leukemia cells shown in **A**. Below quantitative analysis of MEF2C and pS222 MEF2C, as measured using quantitative fluorescence immunoblotting, and normalized to actin, demonstrating significantly reduced abundance of pS222 MEF2C in *Runx1$^{-/-}$;Flt3^{ITD};MEF2C S222A* cells. **C,** Kaplan–Meier survival curves of secondary recipient mice transplanted with wild-type *Runx1$^{-/-}$;Flt3^{ITD};MEF2C*, dominant negative *Runx1$^{-/-}$;Flt3^{ITD};MEF2C S222A* or control *Runx1$^{-/-}$;Flt3^{ITD};MIT* transformed leukemias. N = 10 animals in each group. **D,** Schematic for *in vivo Hoxa9/Meis1* and *MEF2C* initiation/maintenance experiments. **E,** Western blot analysis for MEF2C and Hoxa9 in primary leukemia cells shown in **D**. **F,** Kaplan–Meier survival curves of primary recipient mice transplanted with wild-type *Hoxa9/Meis1;MEF2C*, dominant negative *Hoxa9/Meis1;MEF2C S222A* or control *Hoxa9/Meis1;MIT* transformed leukemias. N = 10 animals in each group. **G,** Colony formation of primary leukemia cells shown in **E**. Error bars represent standard deviation of the mean of 3 biological replicates. **H,** Kaplan–Meier survival curves of secondary recipient mice transplanted with 10,000 cells from that shown in **F**. N = 10 animals in each group.

Supplementary Figure S6.

MEF2C phosphorylation is required for leukemia maintenance and cell survival in MLL-rearranged leukemias

A, Western immunoblot analysis for MEF2C and pS222 MEF2C in human AML cell lines. **B,** Western immunoblot analysis of MEF2C and pS222 MEF2C in MOLM-13, HL-60 and U937 cells lentivirally transduced with wild-type *MEF2C* or dominant negative *MEF2C S222A* transgenes and treated for 48 hours with 600 ng/ml doxycycline to induce transgene expression. Below, quantitative analysis of MEF2C and pS222 MEF2C, as measured using quantitative fluorescence immunoblotting, and normalized to actin, demonstrating significantly reduced abundance of pS222 MEF2C in each case (*,** and *** p = 1.7 x 10^{-6}, 2.5 x 10^{-5} and 1.7 x 10^{-7} for MEF2C S222A versus MEF2C in MOLM-13, HL-60 and U937 cells respectively, t-test). Error bars represent standard deviation of the mean for 3 biological replicates. **C,** Cleaved–caspase 3 analysis in MOLM-13 and OCI-AML2 cells treated with 600 ng/ml doxycycline for 48 hours. Error bars represent standard deviation of the mean for 3 biological replicates. *** and * p = 7.8 x 10^{-5} and 1.3 x 10^{-2} S222A vs MEF2C for MOLM-13 and OCI-AML2, respectively (t-test). **D,** Representative FACS plots of annexin V and DAPI staining in MOLM-13 cells treated with 600

ng/ml doxycycline for 48 hours. **E,** Cell cycle analysis in MOLM-13 and OCI-AML2 cells treated with 600 ng/ml doxycycline to induce transgene expression for 48 hours. Error bars represent standard deviation of the mean for 3 biological replicates. ** and * $p = 2.6 \times 10^{-5}$ and 6.4×10^{-4} S222A versus MEF2C for MOLM-13 and OCI-AML2 S-phase, respectively (t-test). **F,** Representative FACS plots of EdU and PI staining in OCI-AML2 cells treated with 600 ng/ml doxycycline to induce transgene expression for 48 hours. **G,** Western immunoblot analysis for MEF2C and pS222 MEF2C in K562 cells lentivirally transduced with wild-type *MEF2C* or dominant negative *MEF2C S222A* transgenes and treated for 48 hours with 600 ng/ml of doxycycline to induce transgene expression. **H,** Quantitative analysis of MEF2C and pS222 MEF2C, as measured using quantitative fluorescence immunoblotting, and normalized to actin, demonstrating equal expression of MEF2C and MEF2C S222A protein (*$p = 5.1 \times 10^{-2}$, t-test) and significantly reduced abundance of pS222 MEF2C (**$p = 3.1 \times 10^{-3}$ for MEF2C S222A versus MEF2C, t-test). Error bars represent standard deviation of the mean for 3 biological replicates. **I,** Activity of luciferase transcriptional MEF2 reporter in K562 cells shown in **G**. Transgene expression was induced with 600 ng/ml of doxycycline for 48 hours. Error bars represent standard deviation of the mean for 3 biological replicates. * and ** $p = 1.0 \times 10^{-2}$ and 1.6×10^{-2} for un-induced MEF2C versus induced MEF2C and induced MEF2C S222A versus MEF2C respectively, t-test. **J,** Partition around medoid (PAM) clustering of gene accessibility of the most differentially accessible genes by ATAC-seq in OCI-AML2 cells transduced with wild-type MEF2C or dominant-negative MEF2C S222A transgenes (-), and treated with 600 ng/ml doxycycline for 48 hours to induce transgene expression (+). Three biological replicates are shown, as indicated. Blue-to-red color gradient indicates relative accessibility. **K,** Quantitative analysis of MEF2C as measured using quantitative fluorescence immunoblotting, and normalized to actin, of OCI-AML2 cells treated with DSS as shown in Fig. 4I (*$p = 7.9 \times 10^{-4}$, t-test, for S222A vs MEF2C).

Supplementary Figure S7.

Chemical inhibition of MARK/SIK kinases exhibits selective toxicity against MEF2C-activated human AML cell lines

A, Gene expression of *MARK* isoforms in primary AML patient samples from The Cancer Genome Atlas (TCGA). Error bars represent standard deviation of the mean. **B,** *MARK3* gene expression in primary AML patient samples from the TCGA. Data plots represent mean and quartile, with whiskers denoting maximum and minimum values. **C,** Kaplan-Meier survival curves for the Leucegene AML cohort based on the < 75th vs > 75th percentile of *MARK3* expression. $p = 1.7 \times 10^{-3}$, log-rant test. **D,** Western immunoblot for MEF2C, pS222 MEF2C and MARK3 in OCI-AML2 cells lentivirally expressing *MARK3* shRNAs for 6 days. **E,** Hierarchical clustering of gene expression of the most differentially expressed genes in OCI-AML2 cells treated with 100 nM MRT199665 or DMSO for 48 hours. Three biological replicates are shown, as indicated. Blue-to-red color gradient indicates relative gene expression. **F,** Western immunoblot for MEF2C, pS222 MEF2C and MARK3 in MOLM13 cells treated with increasing concentrations of MRT199665 for 12 hours. **G,** Quantitative analysis of MEF2C and pS222 MEF2C abundance, as measured using quantitative fluorescence immunoassays shown in **F**,

and normalized to actin, demonstrating significant reduction of MEF2C phosphorylation by MRT199665 as compared to DMSO control. Error bars represent standard deviation of the mean for 2 biological replicates. **H,** Western immunoblot for MEF2C and pS222 MEF2C in OCI-AML2 cells lentivirally transduced with wild-type *MEF2C* or dominant negative *MEF2C S222A* transgenes and treated for 48 hours with increasing concentrations of MRT199665 and 600 ng/ml doxycycline to induce transgene expression. **I,** Quantitative analysis of MEF2C and pS222 MEF2C abundance, as measured using quantitative fluorescence immunoassays shown in **H**, and normalized to actin (*p = 1.3 x 10^{-2} for MEF2C as compared to DMSO control). **J,** Colony formation of OCI-AML2 cells (red) and U937 cells (black) treated with 10 nM MRT199665 or DMSO vehicle control for 10 days. * p= 2.9 x 10^{-2} (t-test). Error bars represent standard deviation of the mean for 3 biological replicates.

Supplementary Figure S8.

Chemical inhibition of MARK/SIK kinases exhibits selective toxicity against MEF2C-activated primary AML patient cells

A, qRT-PCR of *MEF2C* in primary AML specimens (red) compared to human AML cell lines (black). CN, cytogenetically normal; MLL-r, MLL-rearranged. **B,** Schematic of FACS analysis of patient derived xenograft (PDX) cells treated with MRT199665 for 48 hours. **C,** Cell viability curves as a function of MRT199665 concentration of two MLL-rearranged PDX samples (MSK14 and MSK14) and two normal karyotype PDX samples (MSK21 and MSK54) treated for 48 hours with MRT199665. Error bars represent standard deviation of the mean for 3 biological replicates. **D,** Cell viability curves as a function of MRT199665 concentration in human AML cell lines treated for 48 hours and assessed by FACS of DAPI viability staining in triplicate reactions. Error bars represent standard deviation of the mean for 3 biological replicates.

SUPPLEMENTARY FIGURES

Supplementary Figure 1.

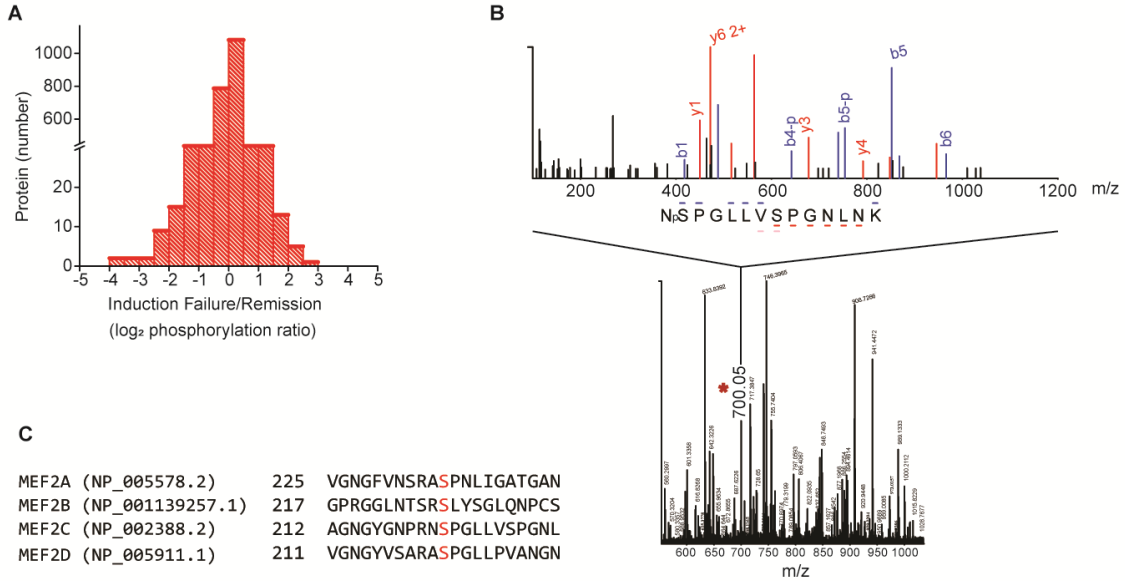

C

```
MEF2A (NP_005578.2)       225  VGNGFVNSRASPNLIGATGAN
MEF2B (NP_001139257.1)    217  GPRGGLNTSRSLYSGLQNPCS
MEF2C (NP_002388.2)       212  AGNGYGNPRNSPGLLVSPGNL
MEF2D (NP_005911.1)       211  VGNGYVSARASPGLLPVANGN
```

Supplementary Figure 2.

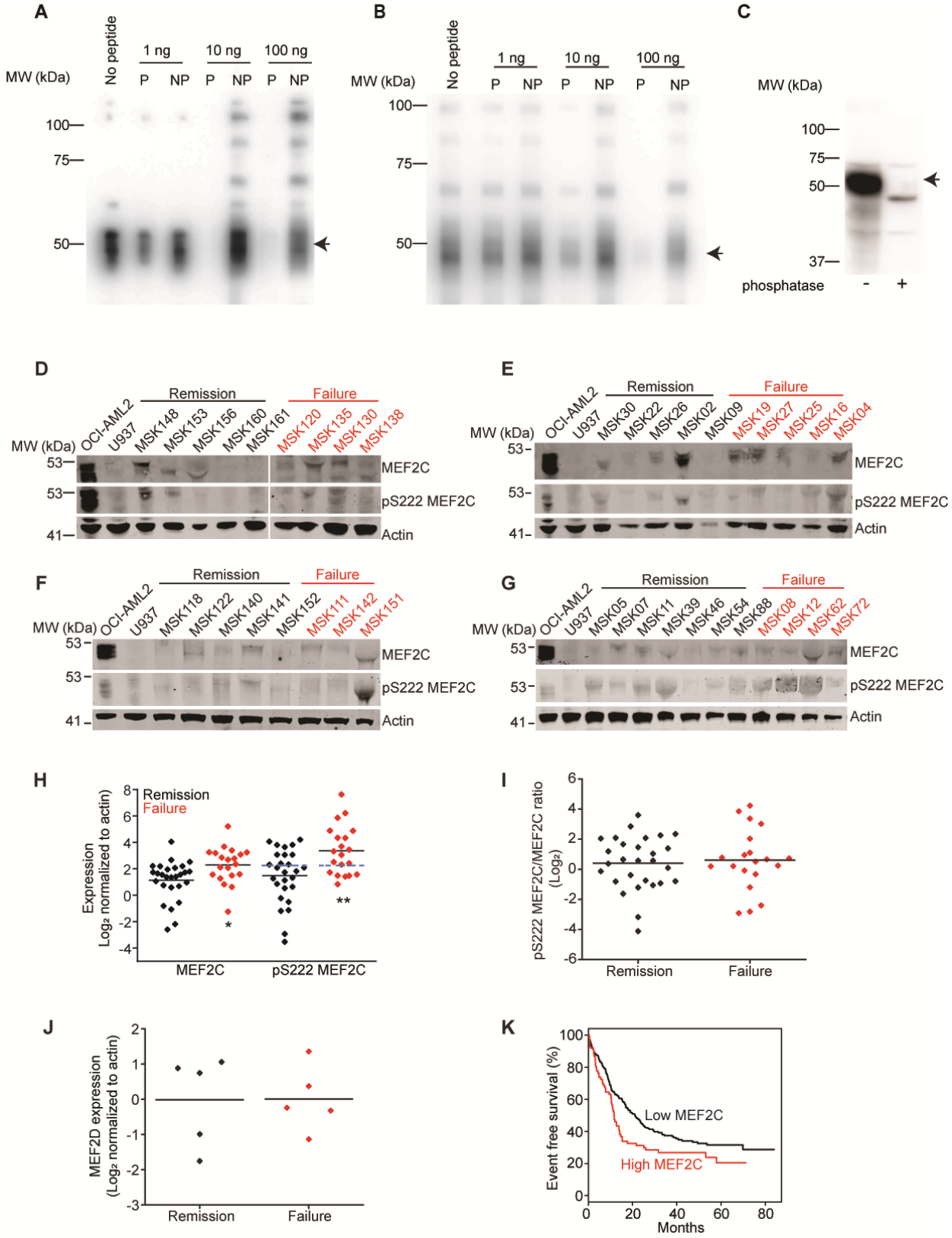

Supplementary Figure 3.

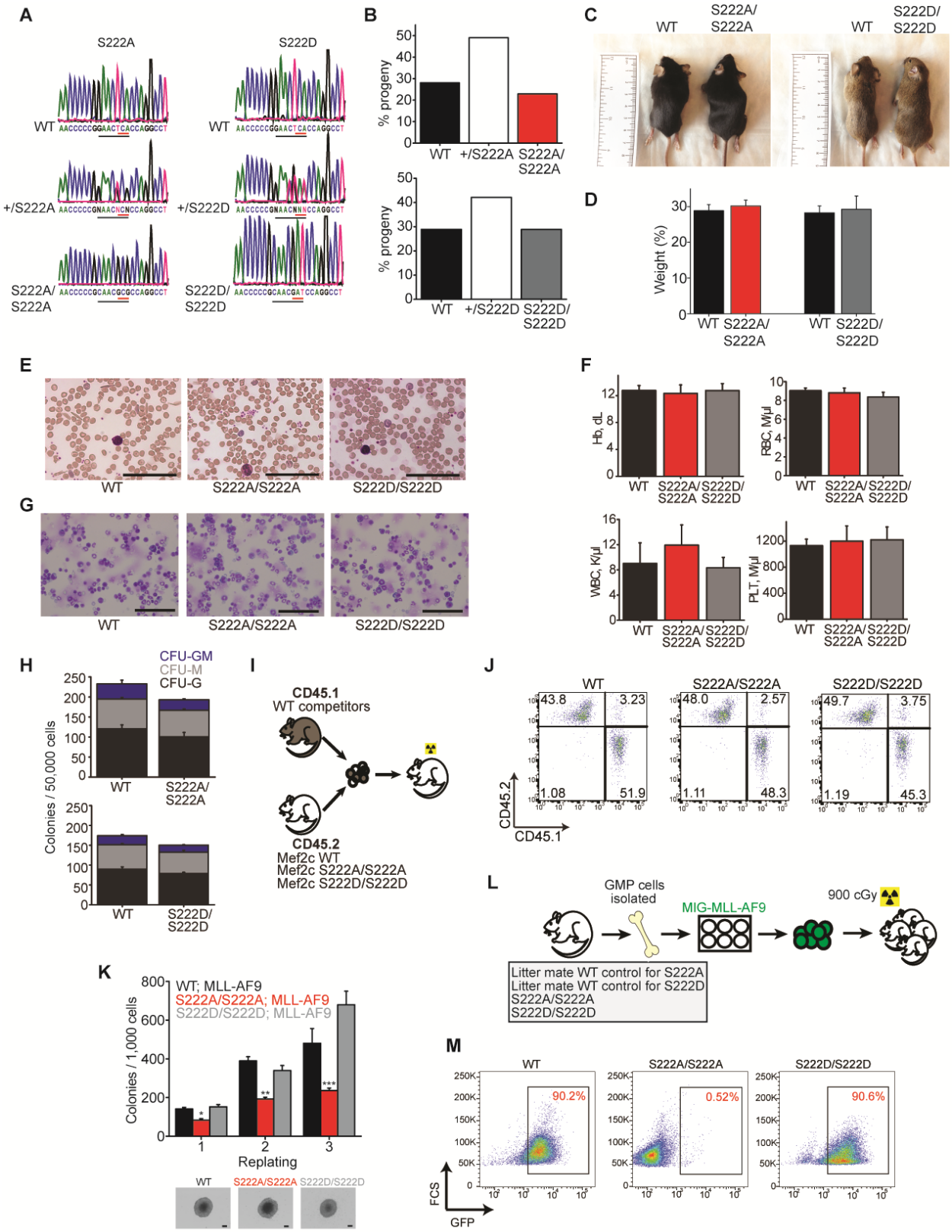

Supplementary Figure 4.

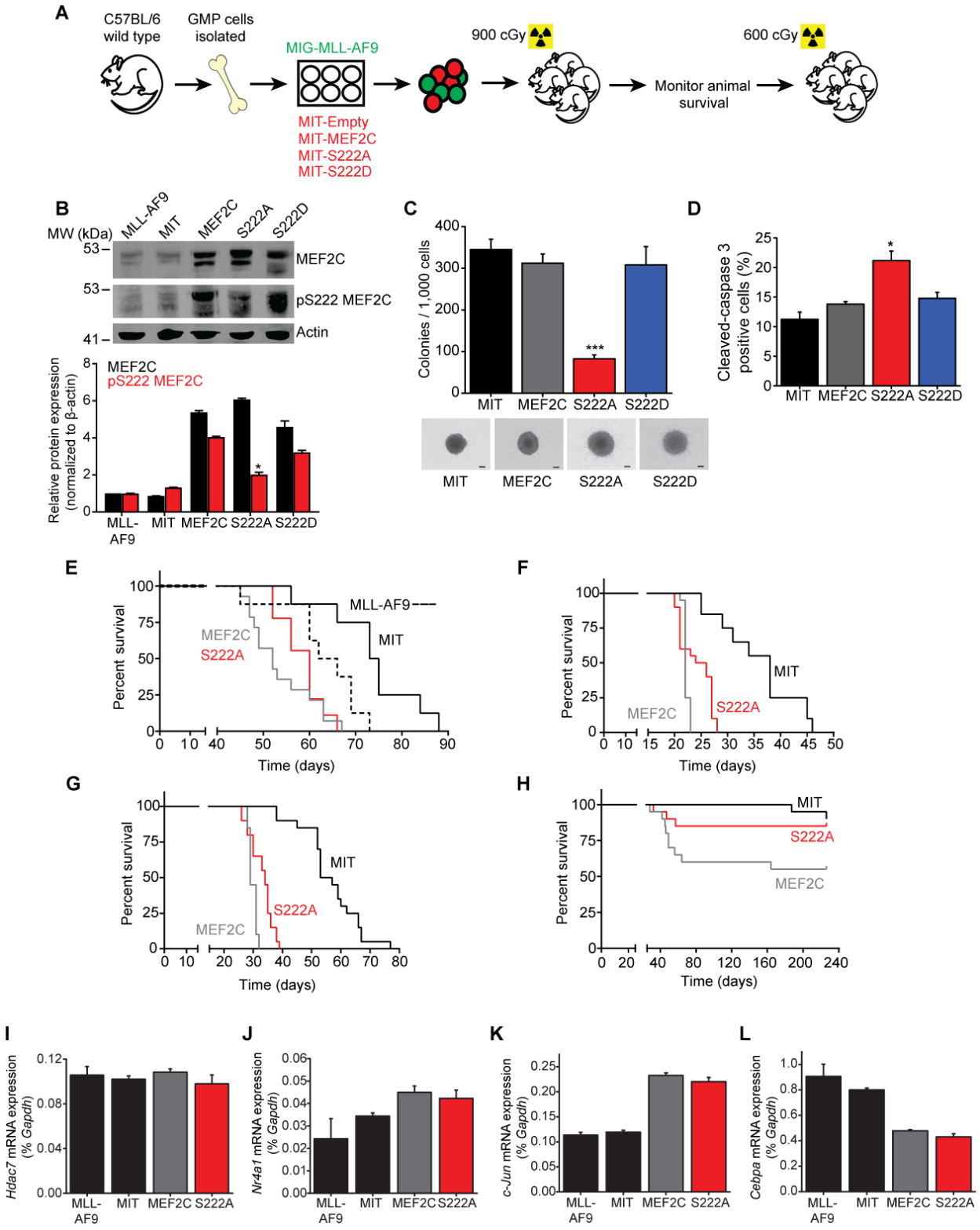

Supplementary Figure 5.

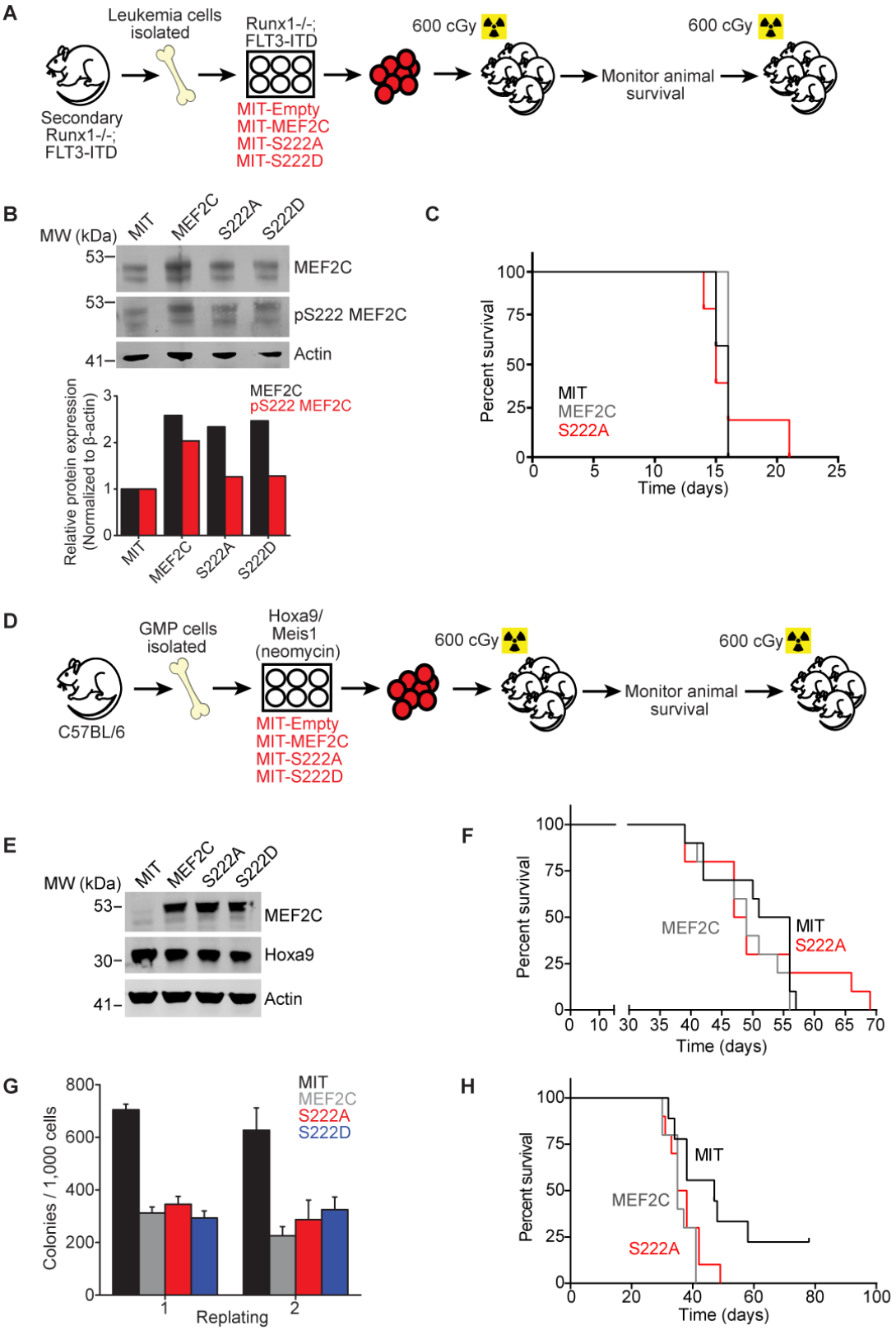

Supplementary Figure 6.

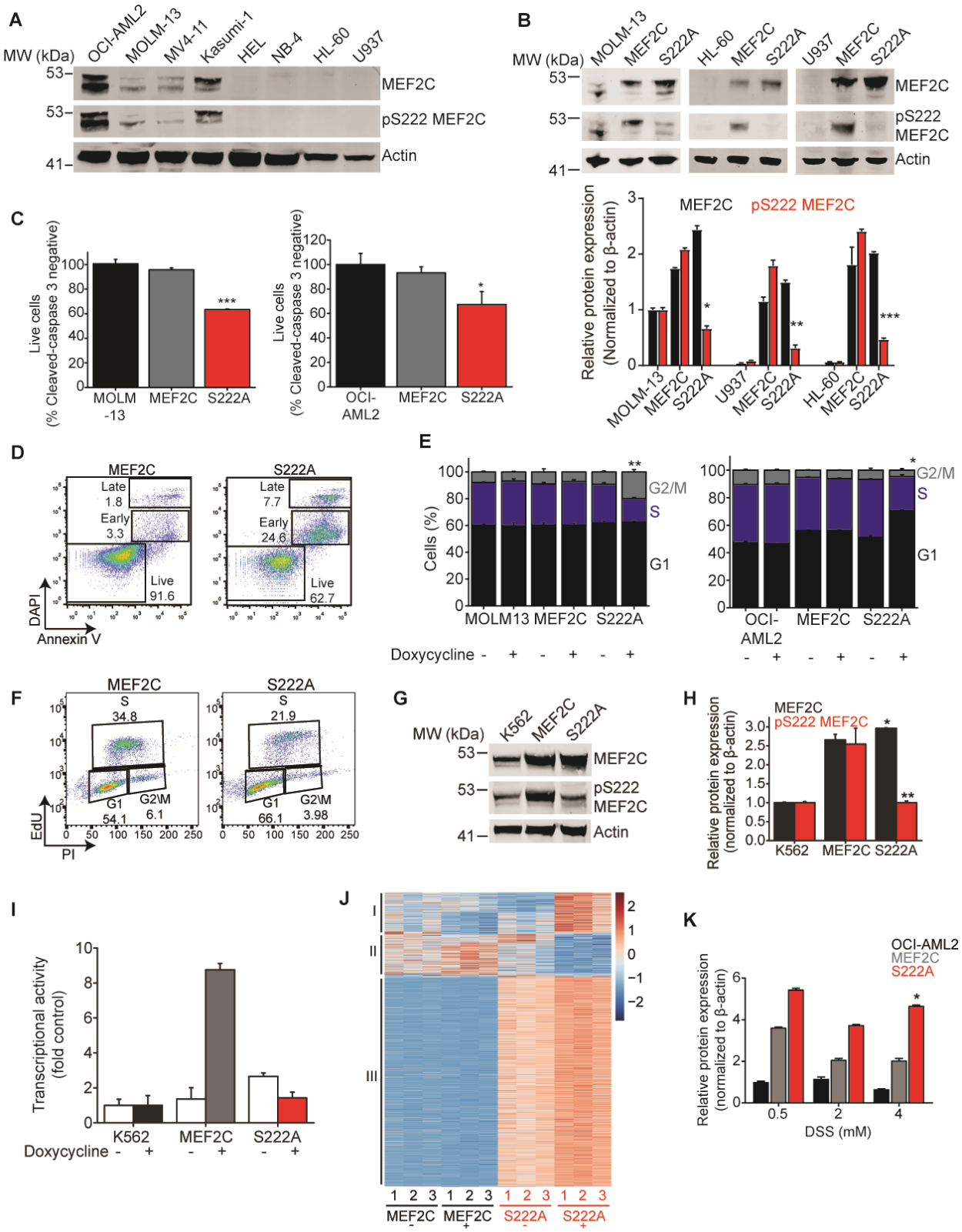

Supplementary Figure 7.

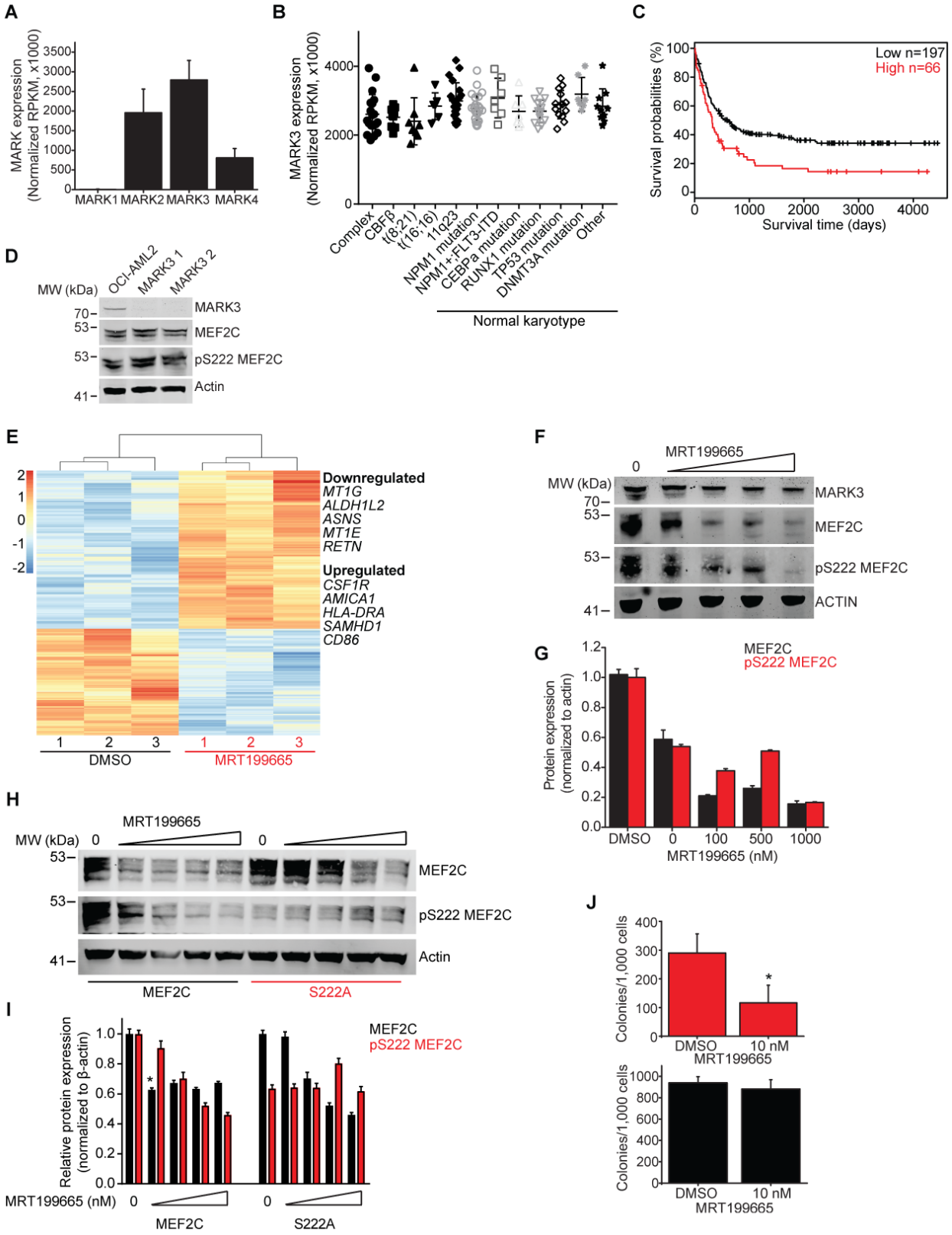

Supplementary Figure 8.

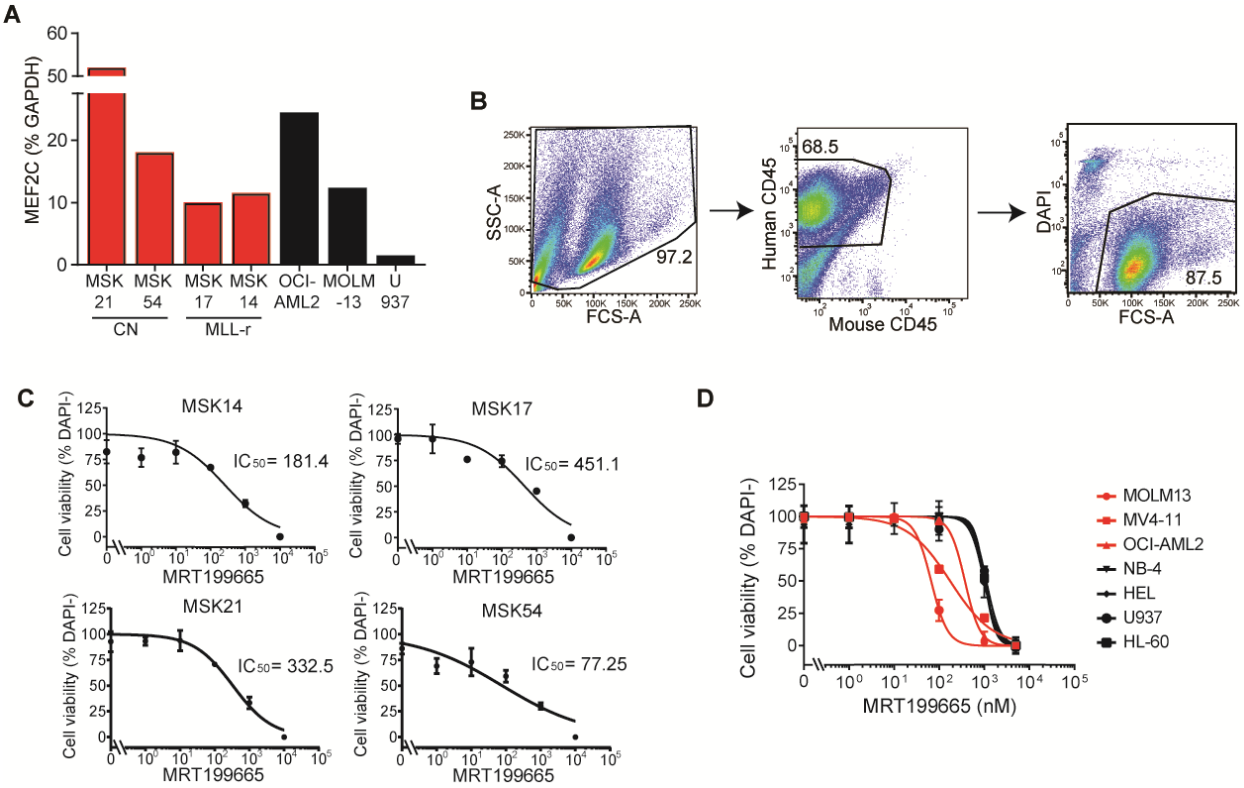

SUPPLEMENTARY TABLES

Supplementary Table S1.

Demographic features of induction failure and induction remission cohorts used for discovery phosphoproteomics

Patient ID	Gender	Therapy outcome	Age (years)	Therapy
59630	M	Failure	59	7+3 DNR and AraC
60438	M	Failure	51	7+3 DNR and AraC
63972	F	Failure	52	7+3 DNR and AraC
56415	F	Failure	44	7+3 DNR and AraC
60376	M	Remission	43	7+3 DNR and AraC
60436	F	Remission	53	7+3 DNR and AraC
60455	F	Remission	66	7+3 DNR and AraC
57878	M	Remission	45	7+3 DNR and AraC

Abbreviations: DNR, daunorubicin.

Supplementary Table S2.

Demographic features and somatic mutations of induction failure and induction remission cohorts used for validation

Patient ID	Therapy outcome	Gender	Age (years)	Therapy	Somatic mutations	Genomic rearrangements
MSK103	Remission	F	7.9	ADE	NRAS_G12D; RUNX1_Q390fs*; FLT3_R595_E596ins;	KMT2A duplication
MSK109	Remission	F	11.4	ADE	WT1_S381fs*4; STK11_F354L; FLT3_G5853_S583ins	
MSK113	Remission	M	16.8	ADE	ND	
MSK110	Remission	F	13.8	ADE	FLT3_T582_G583ins	
MSK106	Remission	M	3.7	ADE	KRAS_G12C; KIT_D816Y; NF2_splice site 1739del	KMT2A_MLLT3 fusion
MSK118	Remission	M	2.9	ADE	NRAS_G12S; ERBB2_P122L; WT1_P376*; FLT3_Q577-M578ins	
MSK122	Remission	M	11.6	ADE	CEBPA_E316-L317ins	
MSK140	Remission	F	15.7	ADE	ETV6_S131fs	NOTCH1_EDF1 truncation; NUP214_SQSTM1 rearrangement
MSK141	Remission	M	12.8	ADE	Fail	
MSK148	Remission	F	17.1	ADE	SETD2_R1625H; WT1_R369*; MDM4_S367L; FLT3_E596_Y597ins	KMT2A duplication
MSK152	Remission	F	8.6	ADE	FLT3_V581-T582ins	
MSK153	Remission	F	16.6	ADE	U2AF1_R156H; YY1AP1_G412S	KMT2A_MLLT4 fusion
MSK156	Remission	M	13.0	ADE	CEBPA_H24fs*; WT1_Q259*; FLT3_V592-D593ins; EP300_splice; CEBPA_T381_S319ins	
MSK160	Remission	M	9.8	ADE	FLT3_Q580-V581ins; CD36_N53fs*; CEBPA_H24fs*	
MSK161	Remission	M	6.6	ADE	CEBPA_Q83fs*; WT1_E150*; ZRSR2_R448-R449ins; CEBPA_T310-Q311ins	
MSK05	Remission	F	50	7+3 DNR and AraC	DNMT3A_R882C; IDH2_R140Q; NRAS_Q61K; NPM1_W288fs*; IDH2_R132H	
MSK07	Remission	F	53	7+3 DNR and AraC	IDH2_R140Q; NPM1_W288fs*	
MSK11	Remission	M	47	7+3 DNR	IDH2_R140Q; FLT3_D835H;	

				and AraC	HNF1A_P568L; NRAS_Q61P; NPM1_W288FS*; CXCR4_L5*; DNMT3A_Q573del	
MSK30	Remission	F	67	IDA+HDAC	FLT3_N676K, S584-S585ins; DNMT3A_P244fs*;	
MSK22	Remission	M	62	7+3 DNR and AraC	NPM1_W288fs*; DNMT3A_R882H; NRAS_G12D	
MSK26	Remission	F	53	7+3 DNR and AraC	DNMT3A_R882H; NPM1_W288fs*; FLT3_Y599ins; TET2_C1281fs*	
MSK02	Remission	F	44	7+3 DNR and AraC	DNMT3A_R882H; EPHA5;R417Q; NPM1_W288fs*; FLT3_G583-S584ins, F590-Y591ins	
MSK09	Remission	F	22	7+3 DNR and AraC	NPM1_W288fs*; EPHA5_R919*; TET2_H434fs*, W564*; FLT3_Y597-E598ins	
MSK39	Remission	M	53	IDA+HDAC	PIK3CG_D238N; NPM1_W288fs*; PTPN11_S502P; IDH2_R140Q; DNMT3A_R882C	
MSK46	Remission	M	31	IDA+HDAC	DNMT3A_R882h; NPM1_W288fs*; FLT3_D835H; FLT3_V592-D593ins	
MSK54	Remission	M	64	IDA+HDAC	EPHB1_V322I; DNMT3A_R882H; NPM1_W288FS*; FLT3_F590_Y591ins	
MSK88	Remission	M	31	FAI	DNMT3A_R635W; NPM1_W288fs*; PTPN11_S502L; FLT3_S584-S585ins; FLT3_R595-E596ins	
MSK104	Failure	F	13.5	ADE	KRAS_G12C	
MSK105	Failure	M	17.6	ADE	FLT3_V579-Q580ins; WT1_A382fs*;	
MSK107	Failure	M	17.2	ADE	DNMT3A_R882H; IDH2_R172K	
MSK108	Failure	F	7.8	ADE	FLT3_S574-Q575ins	
MSK111	Failure	M	13.1	ADE	WT1_A382fs*; FLT3_V592-D593ins	
MSK142	Failure	M	5.9	ADE	WT1_V371fs*; WT1_R370fs*; FLT3_T582-G583ins	
MSK151	Failure	M	15.3	ADE	Fail	
MSK159	Failure	M	10.7	ADE	PTPN11_D61Y; ASXL1_G645fs*	
MSK130	Failure	M	0.8	ADE	NRAS; Q61L; FLT2_D835H; ICK_splice site del	KMT2A_MLLT10 fusion
MSK120	Failure	M	15.8	ADE	FLT3_L610-E611ins; CD36_I399fs*	

MSK138	Failure	M	6.8	ADE	FLT3_T582-G583ins	NSD1_NUP98 fusion
MSK135	Failure	M	18.1	ADE	FLT3_Y591-V592ins	
MSK08	Failure	F	45	7+3 DNR and AraC	DNMT3A_R884H; KRAS_Q61H; FLT3_D835H; PRDM1_K801*	
MSK12	Failure	F	54	7+3 DNR and AraC	TP53_R267Q; NPM1_W288fs*; DNMT3A_R882C	
MSK19	Failure	M	63	7+3 DNR and AraC	DNMT3A_R882H; NPM1_W288fs*; ARID2_Q1149fs*; FLT3_V592-D593ins	
MSK27	Failure	M	55	7+3 DNR and AraC	NPM1_W288fs*; IDH2_R140Q; DNMT3A_splice site	
MSK25	Failure	M	53	7+3 DNR and AraC	DNMT3A_R882H; NPM1_W288fs*; FLT3_R595-F596ins	
MSK16	Failure	F	61	7+3 DNR and AraC	GATA2_R362Q; NPM1_W288fs*; FLT3_Y591ins	
MSK04	Failure	F	50	7+3 DNR and AraC	NPM1_W288fs*; FLT3_R595-E596ins	
MSK62	Failure	M	79	BID FA	NPM1_W288fs*; DNMT3A_R882H; IDH2_R140Q; FLT3_D593-F594ins	
MSK72	Failure	M	51	BID FA	Fail	

Abbreviations: ADE, cytarabine, daunomycin and etoposide-based regimen; IDA, idarubicin; HDAC, high-dose cytarabine; DNR, daunorubicin; BID-FA, twice daily fludarabine + cytarabine; FAI, fludarabine, cytarabine, idarubicin

Table S3A.

Univariate analysis of the validation cohort

Variable	*p* value
Age	0.16
Gender	0.23
DNMT3A	0.74
NPM1	0.92
FLT3	0.94
IDH2	0.82
WT1	0.6
MEF2C	0.01

Table S3B.

Multivariate analysis of the validation cohort

	Hazard Ratio	Lower Limit	Upper Limit	*p* value
Relative pMEF2C expression (Log2)	1.27	1.031	1.56	0.00243
Gender (M)	1.54	0.737	3.2	0.2521
Age (years)	1.00	0.981	1.02	0.9988

Table S4.

Demographic features and somatic mutations of primary AML patients used in patient-derived xenograft (PDX) models

Patient ID	Therapy outcome	Gender	Age (years)	Somatic mutations	Genomic rearrangements
MSK21	Failure	M	51	DNMT3A_R882H; NF1_R1412S; RUNX1_R201Q; FLT3_L610-E611ins	
MSK54	Failure	F	63	DNMT3A_R882H; NPM1_W288fs*; ARID2_Q1149fs*; FLT3_V592-D593ins	
MSK14	Failure	F	42		MLL-AF4
MSK17	Failure	F	61	ECT2L_R852Q; PTPN11_G503A; NRAS_G12S	MLL-AF9

Table S5.
Antibodies

Name	Clone	Catalog #	Source	Technique
Rabbit anti-MEF2C	D80C1	5030	Cell Signaling Technology (CST), Danvers, MA, USA	WB
Rabbit anti-pS222 MEF2C	RRID:AB_2572427	p1208-222	PhosphoSolutions, Aurora, CO, USA	WB
Mouse anti-β-Actin	8H10D10	3700	CST	WB
Rabbit anti-MARK3	--	9311	CST	WB
Mouse anti-LYL1	C-4	Sc-374164	Santa Cruz	WB
Goat Anti Mouse IRDye 800W	--	926-32210	Li-Cor, Nebraska, USA	WB
Goat anti-Rabbit IgG IRDye 680RD	--	925-68071	Li-Cor	WB
APC anti-mouse B220	RA3-6B2	103212	BioLegend, San Diego, CA, USA	FC
FITC anti-mouse Gr-1	RB6-8C5	11-5931-82	eBioscience, San Diego, CA, USA	FC
PE-Cy5 anti-mouse CD11b	M1/70	15-0112-83	eBioscience	FC
Pacific blue anti-mouse CD4	RM4-5	558107	BD Biosciences, San Jose, CA, USA	FC
Pe-Cy7 anti-mouse CD8	53-6.7	25-0081-81	eBioscience	FC
Pacific Blue anti-mouse Sca-1	D7	108120	BioLegend	FC
APC anti-mouse CD117	ACK2	17-1172-83	eBioscience	FC
FITC anti-mouse CD34	RAM34	11-0341-82	eBioscience	FC
PE anti-mouse CD16/32	93	101308	BioLegend	FC
FITC anti-	A20	110705	BioLegend	FC

mouse CD45.1				
Pe/Cy7 anti-mouse CD45.2	104	109829	BioLegend	FC
FITC anti-mouse CD45	30-F11	103108	BioLegend	FC
APC anti-human CD45	HI30	304012	BioLegend	FC
DAPI	--	D1306	Thermo Fisher Scientific, Waltham, MA	FC
APC Annexin V	--	640920	BioLegend	FC
Alexa Fluor® 647 Cleaved Caspase 3	C92-605	560626	BD Biosciences	FC

INDEX FOR SUPPLEMENTARY DATA

Supplementary data files assembled in Brown_etal_SupplementaryData.zip

File number	File name	Description
1	Phosphoproteomics_ITRAQ_Summary.xlsx	Table of phosphopeptides identified in a screen for primary induction failure compared to complete remission AML
2	Transcriptomic and chromatin accessibility profiling. xlsx	Processed data for S222A+ and S222A- cells by RNA and ATAC sequencing
3	Serine threonine kinase screen report.xlsx	Table of results for recombinant protein kinase screen for pS222 MEF2C
4	RNA sequencing for MRT199665 treated cells.xlsx	Processed data for MRT199665 and DMSO treated OCI-AML2 cells by RNA sequencing